International Journal of
INTELLIGENT SYSTEMS AND APPLICATIONS IN ENGINEERING
ISSN:2147-6799 www.ijisae.org Original Research Paper

# Designing and Performance Analysis of a Concentrated Solar Power System in Cold Arid High DNI Area

**C. Vennila[1], G. Muralikrishnan[2], G. Malathi[3], D. R. Srinivasan[4], Ravinaik Banoth[5], J. Immanuel Durai Raj[6]**

**Submitted**: 17/07/2023 **Revised**: 10/09/2023 **Accepted**: 27/09/2023

**Abstract:** The study focuses on concentrated solar power (CSP) technology, a promising development in solar energy application. Unlike photovoltaic (PV) systems, CSP offers potential advantages with higher efficiency. The objective is to analyze the design and thermal performance of a 10 MW solar tower power (STP) plant, coupled with 10 hours of thermal energy storage, in the Leh region. The aim is to assess the viability of CSP technology in cold arid areas with high direct normal irradiance (DNI).The System Advisor Model (SAM) is used to simulate the 10 MW STP plant in the Leh region. SAM is a widely used software for techno-economic analysis of renewable energy systems. The design, thermal aspects, and integration of thermal energy storage are considered. Meteorological data, including annual DNI, are incorporated to model the plant's behavior under real-world conditions and evaluate various performance parameters and economic factors.The analysis demonstrates promising results for the CSP plant in Leh. The calculated capacity factor (CF) is 56.90%, indicating high electricity generation capacity compared to its rated capacity. The plant efficiency is measured at 16.35%, highlighting the effectiveness of the solar thermal technology used. The levelized cost of electricity (LCOE) is determined to be 0.1202 $/kWh, showcasing the economic viability of the CSP plant in the selected location. These results indicate the potential of CSP technology to efficiently harness solar energy in cold arid regions with high DNI.The research on the 10 MW STP plant in Leh reveals promising findings for concentrated solar power (CSP) technology. The study emphasizes the advantages of CSP over traditional PV systems, particularly in cold arid regions with high DNI. The plant's high capacity factor, efficiency, and economically viable LCOE make it a suitable option for expanding solar thermal power in such areas. The successful design and performance analysis of the CSP plant offer valuable insights into the feasibility of implementing solar thermal power solutions, contributing to global efforts to transition towards sustainable and renewable energy sources.

***Keywords:*** *Solar thermal power, DNI, Power plant performance, Heat transfer fluid, Economic analysis.*

## 1. Introduction

The availability of affordable, reliable energy sources is essential to the growth of any economy. As the world's population and quality of life continue to rise, so too does the demand for energy [1]. Distribution and progress of the different power generation techniques from the renewable energy sources are being given more attention in order to meet the mounting worldwide requirement for electric energy in an environmentally friendly manner. One of the most important renewable energy sources, solar power will likely account for a sizable portion of the total energy produced in the near future [2]. Solar PV and solar thermal technologies are both viable options for collecting solar energy. The use of PV technology to generate electricity is currently widespread across the globe. Globally, PV solar power accounts for more than 98 percent of the solar power generation, while CSP generation accounts for the less than 2 percent of solar power generation [3]. Despite solar energy's vast potential, both technological avenues rely heavily on consistent exposure to sunlight. Concentrated solar power plants require high levels of direct normal irradiance (DNI) in order to work properly, while photovoltaic (PV) systems may generate electricity from the sun using both DNI and diffuse solar radiation [2]. Only in the high sun radiation belt is CSP plant is possible. CSP plants may only be established in locations with the daily direct solar irradiance is equal or greater than 5.5 kWh/m$^2$ [4,5]. Few researchers estimate threshold values of yearly DNI of 1800 kWh/m$^2$/day and 2000 kWh/m$^2$/day for concentrated solar power generation [1,6,7,8].

### 1.1 Scope of the study

The paper's authors discuss that widespread adoption of solar PV and solar thermal (ST) power production

[1]*Department of Electrical and Electronics Engineering Alagappa Chettiar Government College of Engineering and Technology, Karaikudi-630003, Tamil Nadu, Email: c.vennila.acgceteee@gmail.com*
[2]*Department of Electrical and Electronics Engineering ,S.A.Engineering College, Chennai, India Email: murtkg14787@gmail.com*
[3]*Department of Electrical and Electronics Engineering M. A. M School of Engineering,Siruganur, Trichy- 621105. Email: ursermala@gmail.com*
[4]*Department of Mechanical Engineering, JNTUA College of Engineering (Autonomous) Ananthapuramu, Andhra Pradesh-515002, INDIA Email:drsrinivasan.mech@jntua.ac.in*
[5]*Department of Mechanical Engineering, St. Martin's Engineering College, Secunderabad, Telangana, India, Email: ravi304banoth@gmail.com*
[6]*Department of Mechanical engineering, St. Joseph's Institute of Technology, OMR, Chennai 600119, India. Email: immanuelje74@gmail.com*

technologies is crucial to the future of solar power. With the PV industry's manufacturing prices falling quickly as a result of mass production and related learning curves, the solar thermal power sector has recently experienced intense competition [9]. Solar thermal only makes up a tiny portion of the worldwide solar power generating scenario as things are right now. Since solar thermal power generation offers several intrinsic benefits, such as energy dispatchability through the thermal storage, higher power plant efficiencies, reduced the plant investment costs, and superior hybrid competability with other fuels, it is essential to concentrate more on the technology if land is not a restriction [10]. Concentrated solar energy plants are typically thought to need a lot of DNI and are finest built in semi-arid or dry areas [11].

It is projected that Ladakh's demand for electricity would expand to 140.5 MW by 2025, a rate of increase of 7% per year. Diesel fueling the power plants that provide Ladakh with its daily electricity needs now requires the import of 8,000 litres. The Ladakh Renewable Energy Development Agency (LREDA) is working tirelessly to increase the region's reliance on renewable energy sources, and it serves as the coordinating body for the MNRE, Government of India's non-conventional energy projects in Ladakh. Connecting the transmission lines with a centralised grid system are neither physically viable nor economically feasible as a means of bringing electricity to rural places, and doing so during the winter is an especially difficult problem. Ladakh has access to a wide variety of green and alternative energy sources, although radiation energy from sun is by far the most powerful. The country's dry and semi-arid regions get significantly more sunlight than the rest of the country. Leh-Ladakh, in the country's cold desert area, receive the most radiation, is almost 7–7.5 kWh/m$^2$/day. Since the Leh Ladakh region of India receives an exceptionally high quantity of solar radiation, there has been a lot of potential for expansion in the solar power industry in this area [12]. An average of 2396.79 kWh/m$^2$ of DNI is received annually by the area. The Leh Ladakh region has such a great potential for solar radiation; thus, it should serve as the primary location for a electric power plant based on solar radiation that uses concentrated solar technology. The resolution of this research is to investigate the possible of solar thermal power generation in this cold arid and high DNI area in India.

The research objectives are segregated in these below segments

- To determine the feasibility for CSP plant in the Leh-Ladakh region.
- To design and simulate STP with the support of NREL weather record and SAM software.
- To analyze the performance investigation of the hypothetical CSP technology with STP technology integrated with TES.

### 1.2 Details landscape of the plant location

India enjoys a plenty of energy from sun due to the country’s location in the equatorial zone. DNI in most of India is between 4 and 5 kWh/m$^2$/day [13], and the country's land area receives about 5,000 trillion kWh annually. As a part of India, Ladakh shares its eastern border with the Tibet Autonomous Region, its southern border with Himachal Pradesh, its western border with Indian state Jammu and Kashmir, and its northernmost border with the southwest portion of Xinjiang via the Karakoram Pass. From the northern Siachen Glacier in the Karakoram range to the southern Great Himalayas, this range covers a vast area. Leh serves as the co-capital of the Ladakh region and is its largest city. Leh, in the Leh district, is not only the current capital of Ladakh but also its ancient capital. Located at an elevation of 3,524 metres (11,562 feet), the city of Leh is linked to the cities of Srinagar, located to the southwest, and Manali, located to the south, by the National Highway 1 and the Leh-Manali Highway, respectively. There is a wide variation in the average rainfall in the state, from 3.6 mm to 15.4 mm [14].

### 1.3 Brief literature review

Concentrating solar power (CSP) potential and methods to advance this technology in China has been investigated by Hang et al. [15]. A huge CSP plant at Wilayat Duqum, Oman, which gets exceptionally strong solar radiation throughout the year, is evaluated by Charabi and Gastli [16]. A complete economic analysis of solar thermal energy generation in some sites in India has been conducted by Purohit and Purohit [1]. Arora [11] looked at the viability of CSP plants in the Thar Desert area of Rajasthan, India. TES system included in CSP facilities has been surveyed by Kuravi et al. [17]. A prospective valuation of solar thermal plants for energy production in West Africa has been reported by Ramde et al. [18]. Receiver efficiency in STP plants has been studied by Benammar et al. [19], who looked at how factors like surface area and temperature affected performance. A hybrid concept of the solar through and gas turbine has been designed by Turchi and Ma [20] to improve solar thermal plant power production efficiency while dropping gas heat rate. The method for optimising the spreading of the solar flux on the receiver surface which is concentrated by the solar field mirror has been devised by Yu et al. [21]. Boudaoud et al. find the feasibility of a STP plant in Algeria [22]. An active simulation of a STP plant of 1 MW size with TES has been done by Liu et al. [23]. Using a variety of methods, Mutuberria et al. [24] analysed the efficiency of a central receiver based CSP plant's heliostat solar field arrangement. CSP plant power generation in

Indian region has been evaluated by Sharma et al. [2] where the DNI values are ranges from 1800 kWh/m$^2$/year and 2000 kWh/m$^2$/year. When solar irradiation is high enough, Santos et al. [25] have analysed the performance of a hybrid plant (solar and gas turbine) and made a regular thermodynamic forecast. In order to learn how well solar thermal parabolic trough power plants operate in the dry/arid region with high DNI of southern area of Tunisia, by Trabelsi et al. [26]. Astolfi et al. investigated many alternative optimization techniques of STP plant in Seville region of Spain [27]. The performance analysis of a 100 MW CSP plant based on parabolic trough system has been assessed by Bishoyi and Sudhakar [5] for a site in Rajasthan, India, where the DNI value is 2248.17 kWh/m$^2$/year. Bhattacharjee and Bhattacharjee [28] find the possibility of the CSP plant in low DNI condition. Bhattacharjee and Bhattacharjee [29] analysed the different plant design parameter and find out the best combination of the designing parameter to get better result from the CSP plant in the low DNI region. To achieved higher efficiency from the TES Lisbona et al. [30] designed and analysed the performance of both two multi-stage solar calcination and one-stage isothermal calciner under various test conditions. A novel designed of hybrid TES and operation plans has been done by Ma et al. [31] for CSP plant. Middelhoff et al [32] designed and analysed the techno-economic performance of the hybrid CSP and biomass plant for powe generation in the Australian location and also find the environmental impact. Coutinho et al. [33] investigated the thermo-economic performance of hybrid solar thermal power plant and also optimized the plant using genetic algorithm. Tiwari et al. [34] have done a parametric optimization and analysis of a latent heat TES system for CSP plant under various real operating situations. Boukelia et al. [35] compared the thermodynamic performance analysis of convetional solar tower plant with hybrid solar tower plant and geothermal power plant. Liu et al. [36] investigated the thermal performance of latent and sensible TES system for CSP plants. García-Ferrero [37] have done a comparative analysis of parabolic dish farms and central tower plants performance.

## 2. CSP Plant Process

The current research is based on the hypothesis that a STP plant will prove to be an effective Concentrating Solar Power (CSP) technology. With the meteorological conditions in Leh, northern India, the proposed plant's capacity has been set at 10 MW. The power plant's functioning is depicted in Figure.1, and the design features taken into account during plant profiling are listed in Table 1. There are four main sections of the STPP those are the solar field which is known heliostat section, the receiver section placed at the field centre, the steam production section, and the power cycle section. The heliostat section is made up of a thousand of concentrated mirrors that focus the sun's flux on the receiver surface situated at the top of central tower. With the use of a heliostat's canting on a single axis, the mirrors can be brought into focus. A molten salt mixture of 40% $KNO_3$ and 60% $NaNO_3$ is utilised as the heat transfer fluid in an external cylindrical receiver. Heliostat mirrors capture solar energy by concentrating the solar rays on a single receiver surface at the topmost of a tower. With enough concentrated solar energy on the receiver's outer surface, molten salt is heated to a very high temperature. Thermal energy is transmitted from the surface of cavity receiver to the steam generation portion by using heated molten salt. The HTF at cavity receiver is approximately 565 ℃ in temperature. Pumping water serves as the working fluid in the steam generation unit. Water in the steam generator subsystem absorbed the heat delivered by the HTF, creating superheated steam at temperatures in the range of 552 ℃. The steam is then utilised to power a turbine generator, which in turn generates electricity. Once the molten salt has cooled down in the steam generator, it is then send to condenser and then send again to the top of the tower to collect heat from the surface of the receiver to begin the next cycle [19].

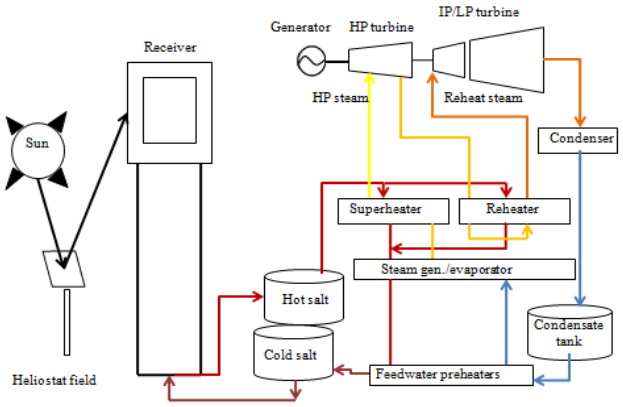


**Fig..1** Schematic diagram of STP plant [29]

**Table 1** Plant profile assumption

| Plant input | Value |
|---|---|
| Climate details | |
| Site longitude | 77.55 °E |
| Site latitude | 34.15 °N |
| Temperature | -22 to 21 $^0$C |
| Beam radiation (DNI) | 2396.79 kWh/m$^2$/year |
| Wind flow rate (mean) | 2.3 m/s |
| Heliostat field profile | |
| Single mirror aperture area | 36 m$^2$ (6×6) |
| Heliostat canting method | On-axis |

| | |
|---|---|
| Focusing method of Heliostat mirror | Ideal |
| Heliostats count | 3316 |
| Land area (not include solar field) | 2 acres |
| Total plant area | 108 acres |
| Central tower and cavity receiver profile | |
| Height of the central tower | 115 m |
| Receiver height | 8 m |
| Receiver diameter | 4 m |
| Solar multiplier | 2.4 |
| Number of panels | 16 |
| Heat loss in receiver | 30 $kW_t/m^2$ |
| Maximum flux on the receiver surface | 1000 $kW_t/m^2$ |
| Receiver flux map resolution | 16 |
| Maximum fraction of the receiver operation | 1.2 |
| Statup energy delay fraction of the receiver | 0.25 |
| Time required to receiver startup | 0.2 h |
| Tube outer diameter | 25 mm |
| Required HTF outlet temperature | 565 $^0C$ |
| Coating emittance | 0.88 |
| Thickness of the tube wall | 1.25 mm |
| HTF outlet temperature | 565 $^0C$ |
| HTF Inlet temperature | 250 $^0C$ |
| Coating absorptance | 0.94 |
| HTF type | Salt 60% $NaNO_3$40%$KNO_3$ |
| TES | |
| TES (hours for full load) | 10 hr |
| Tank heater efficiency | 0.99 |
| Cold tank heater temperature | 230 $^0C$ |
| Storage tank volume | 1089 $m^3$ |
| Power block profile | |
| Gross output from turbine | 10 MW |
| Net design output (nameplate) estimated | 8.5 MW |
| Technology of the power cycle | Rankine cycle |
| Pressure at boiler | 100 bar |
| Control process of the input pressure of the boiler | Fixed pressure |
| Type of the condenser | Air-cooled |
| HTF inlet temperature | 250 $^0C$ |
| HTF outlet temperature | 565 $^0C$ |
| Cycle thermal efficiency | 0.425 |
| System cost | |
| Heliostat field | 200 $\$/m^2$ [38] |
| Site improvement | 20 $\$/m^2$ [38] |
| Power block | 550 $\$/kW_e$ [22] |
| Balance of plant | 420 $\$/kW_e$ [22] |
| Tower cost | 12.8 $M |
| Land cost | 78050 $/acre |
| Tower cost | 12.8 $M |
| Storage | 30 $\$/kW_{ht}$ [22] |

## 3. Related Equation and Parameter Description

### 3.1 DNI profile

Information on solar resources with a spatial resolution and high sequential is essential for all stages of a solar power generation power plants, from basic formulation through everyday solar power plant operations. As an example, SAM uses information about solar resources and weather as inputs to predict system performance and costs. The solar radiation database has been developed by the NREL of the energy department of the US. The data collection is accessible to the public and has served as the premier solar energy resource and meteorological data from the different weather station for various nonconventional energy applications. National solar radiation database (NSRDB) is used to provide the most accurate picture possible. Half-hourly sequential resolution and high resolution DNI data from NSRDB has been used in this study. Using a physics-based technique in which various atmospheric variables are collected from satellite resource and utilized as an input in the different calculation model to easure the surface solar radiation, the current NSRDB (1998-2015) has been constructed [39]. Libraries for the SAM incorporate TMY data in csv format. The area's DNI profile is depicted in

Figure. 2. Figure 2 shows that during the months of September, October, November, and December, the DNI values are at their highest right around solar noon. The atmospheric temperature of the study location is one of the most key parameter that give some influence on the efficiency of the STP plant. The mean atmospheric temperatures throughout the year are displayed in Figure. 3. According to the data, the average temperature at the site under investigation ranges from -22 ° C to 21 ° C.

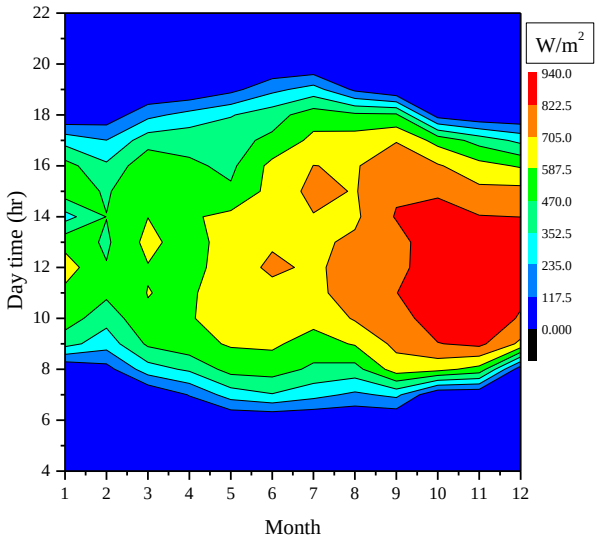


**Fig. 2.** Monthly hourly average DNI values

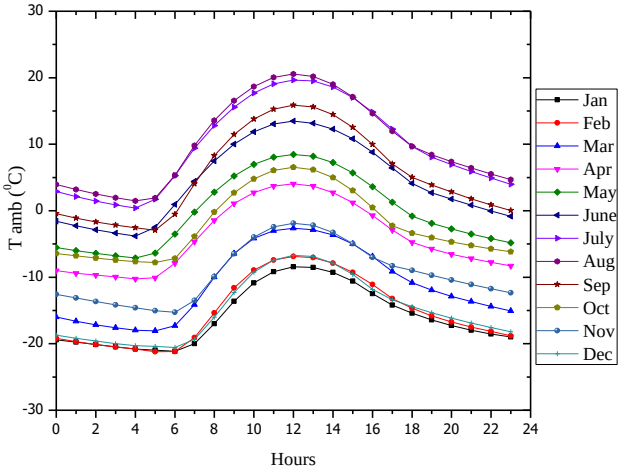


**Fig. 3.** Ambient temperature profile

### 3.2 Platform for the simulation

In this work, SAM has been used a package created by the US Department of Energy's NREL, to formulate the technical details of a power plant that generates electricity from solar thermal sources. SAM's emphasis on system performance and economic modelling creates robust analysis tools for energy experts. When it comes to software platforms for CSP system modelling, SAM is by far the most often used option. Using the information in this database, customers may more easily establish the settings for an entire project. There are a number of interrelated parts to the model. Additionally, each part can be characterized by different variables and inputs which are time dependent, which in turn gives various time-dependent outputs. One component's output may serve as input for another component or for the system as a whole [26].

### 3.3 Mathematical formula

#### 3.3.1. Formulation of solar tower plant.

The four major components of the STP plant has been described below.

##### 3.3.1.1. Solar field subsystem

There are several mirrors in the solar field. The mirror on the heliostat directs the incoming sunlight toward the receiver. The heliostat field transmits ($Q_{re}$) some percentage of the incident DNI $Q_h$ to the receiver, while the rest $Q_o$ is missing to the atmosphere via different loss processes [19].

The mathematical formula is given as:

$$Q_h = Q_{re} + Q_o \quad (1)$$

The optical efficiency of a heliostat solar field may alternatively be described as the percentage of incident solar power that is converted to useful usable heat by the receiver surface ($Q_{rec}$). [22].

$$\eta_{opt} = \frac{Q_{rec}}{I_d \times N_h \times A_h} \quad (2)$$

$A_h$ denotes heliostat mirror total surface area ($m^2$), $I_d$ is the DNI and $N_h$ define the entire mirrors present in the heliostat field.

##### 3.3.1.2. Receiver formulation

The CSP is used the receiver to transmit energy to the HTF in terms of thermal power. A portion of the heat from the receiver ($Q_{re}$) is passed to the molten salt, which is the HTF ($Q_{re,abs}$). Losses due to convection ($Q_{con}$), heat losses due to radiation ($Q_{rad}$), loss due to reflection ($Q_{ref}$), and heat loss due to conduction ($Q_{cond}$) all contribute to the total amount of environmental losses heat energy lost ($Q_{re,totloss}$) [19]. Therefore,

$$Q_{re,totloss} = Q_{con} + Q_{rad} + Q_{ref} + Q_{cond} \quad (3)$$

The receiver thermal efficiency is denoted by $\eta_{re}$, and is calculated as $Q_{re,abs}/Q_{re}$, where $Q_{re,abs}$ is the amount of

thermal energy absorbed by the HTF and $Q_{re}$ is the amount of thermal energy incident on the receiver absorber surface ($Q_{re}$) [40].

$$\eta_{re} = \frac{Q_{re,abs}}{Q_{re}} \quad (4)$$

The energy balance equation:

$$Q_{re} = Q_{re,abs} + Q_{re,totloss} \quad (5)$$

To determine plant power generation with constant receiver thermal efficiency, the HTF maximum mass flow rate inside the central receiver is considered as an important variable. In order to compute the receiver thermal efficiency, the maximum mass flow rate has been given below [41]:

Maximum flow rate to receiver = (Receiver thermal power (MWt) × Maximum receiver operation fraction × 1,000,000) ÷ (HTF Specific heat × 1,000,000 × (HTF temperature $^0$C (hot) - HTF temperature $^0$C (cold))) (6)

**3.3.1.3. Steam generation section (SGS)**

CSP plant's critical steam production section connects solar flux receiver to steam turbine via heat exchangers, heating HTF to generate steam. [19].

**3.3.1.4. Power block unit**

The Rankine cycle consists of a feed-water heater, pumps, a condenser, and high & low pressure turbines. Steam energy (Qst,abs) is converted to mechanical energy (Wnet) in the turbine, driving a generator for electricity production [19]:

$$Q_{st,abs} = W_{net} + Q_{ps,totloss} \quad (7)$$

The relationship between the heat fed into the power cycle and the power generated as a function of the HTF temperature, condenser pressure, and HTF mass flow rate.The corelation between the thermal efficiency of the HTF cycle, the rate at which heat is absorbed by the HTF cycle, and the output temperature of the HTF , as shown below. [28]:

$$T_{htf,out} = T_{htf,in} - \frac{Q_{ab}}{\dot{m}_{htf}\, c_{htf,avg}} \quad (8)$$

$$\eta_{cycle} = \frac{\dot{W}}{Q_{ab}} \quad (9)$$

$\eta_{cycle}$ is power cycle efficiency with $T_{htf,out}$ and $T_{htf,in}$ as outlet and inlet HTF temperatures, $\dot{m}_{htf}$ as mass flow rate, $c_{htf,avg}$ as average specific heat, $\dot{W}$ as cycle power output, and $Q_{ab}$ as cycle heat absorption rate.

**3.3.2. Capacity factor (CF)**

CF is defined as the proportion of the actual energy produced at partial load to the potential energy produced if the plant is run at full load. [22].

$$CF = \frac{E_{net}}{C_{design} \times 8760} \times 100 \quad (10)$$

Where, the yearly total energy generation is defined by $E_{net}$ which unit is kWh/year, and $C_{design}$ as the nameplate capacity of solar thermal power plant is which unit is kW.

**3.3.3. Solar multiple (SM)**

The SM is the ration of the total thermal power produced by the heliostat field and the total thermal power required in the power block [22].

$$SM = \frac{q_{sf}}{q_{pb}} \quad (11)$$

Where is thermal power generated by the solar field is defined by $q_{sf}$ ($kW_{th}$) and the total thermal power required in the power block at nominal conditions is defined by $q_{pb}$ ($kW_{th}$).

**3.3.4. Levelized cost of energy (LCOE)**

LCOE defines the yearly cost of one unit of energy generating. [42, 43].

$$LCOE = \frac{\sum_{n=0}^{N} \frac{C_n}{(1+d)^n}}{\sum_{n=1}^{N} \frac{E_{net}}{(1+d)^n}} \quad (12)$$

$E_{net}$ (kWh) is electricity produced by the power plant in year n,
N is the total period of analysis in years,
$C_n$ is the annual project costs in year n, d is the nominal discount rate.

## 4. Results and Discussions

### 4.1 Solar multiple

Figure 4 demonstrates the influence of SM on a power plant. Higher TES and SM result in increased CF and plant efficiency. For instance, a TES of 10 hrs and SM of 2.4 yield a 16.35% plant efficiency.

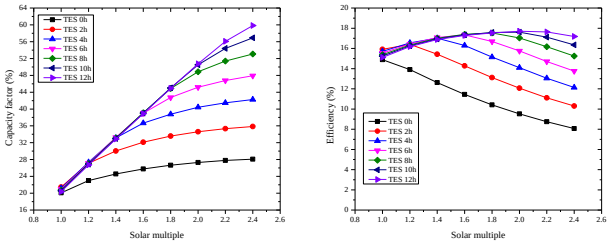


(a) Impact of SM on the capacity factor for various TES values

(b) Impact of SM on the plant efficiency for various TES values

**Fig. 4.** Impact of SM on the plant CF and STP efficiency

### 4.2 TES performance

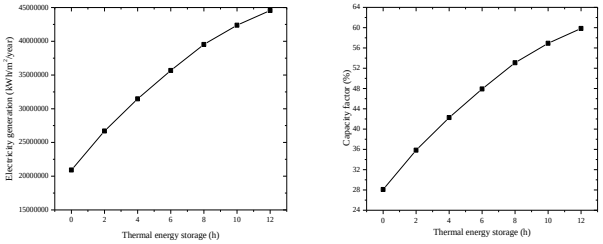


(a) Impact of TES on the plant electricity production

(b) Impact of TES on plant capacity factor

**Fig.5.** Impact of thermal energy storage

TES enables long-term operation of CSP power plants by storing solar energy in thermal forms. Figure 5(a) shows yearly electricity generation, peaking at 44.56 GWh for TES=12h. Figure 5(b) indicates plant CF rising from 56.90% (TES=10h) to 59.82% (TES=12h).

### 4.3 Receiver performance analysis

Figure 6(a) depicts how increased thermal power incident on the receiver surface enhances central receiver thermal efficiency. Figure 6(b) shows the yearly variation in receiver thermal power relative to HTF in the CSP plant.

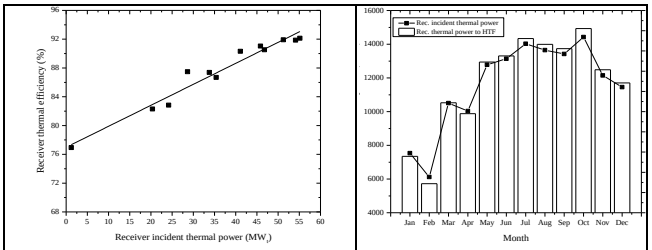


(a) Incident thermal power on the solar receiver with receiver thermal efficiency.

(b) Receiver input and output thermal power

**Fig. 6.** Receiver thermal property characterization

### 4.4 Power plant daily average performance

Power plant daily average performance for four typical days (one day of March, one day of June, One day of September and one day of December selected) are shown in Figure.7. These months day has been taken because the earth sun geometry has four special days. Out of these four days, two equinox days on March and September when the Earth declination angle is zero, one day is on June when the Earth declination angle on the Norther hemisphere is highest which is 23.5 degree and one day is on December when the Earth declination angle on the Norther hemisphere is lowest which is -23.5 degree.

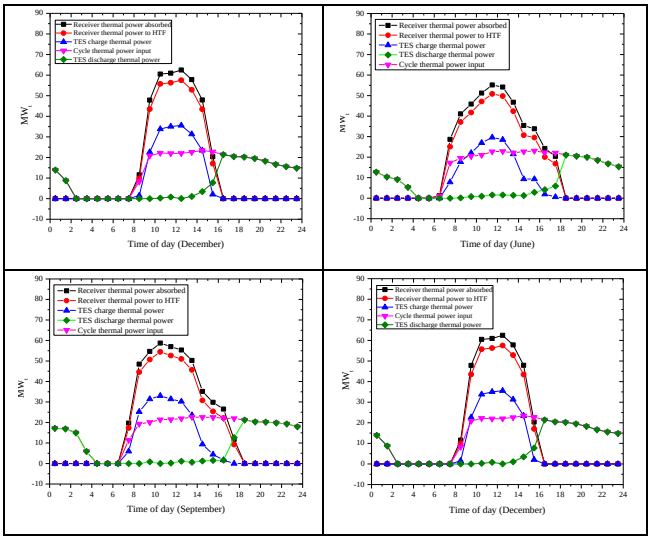


**Fig. 7.** Plant performance for a day

### 4.5 Impact of the CSP capacity on the CSP performance

Figure.8 displays the importance of the power plant capacity on the CSP performance. Figure.8 (a) displays the influence of plant capacity on the CSP CF. From the graph it has been shown that the 10 MW power plant gives the higher plant capacity factor compared to the other plant size in that limited land area. Figure. 8(b) displays that with the rise of the CSP size the solar field area of the power plant will become more. Figure. 8(c) express that the increase of the CSP capacity the electricity generation of the CSP is become more. Figure. 8(d) shows the plant solar to electricity efficiency with plant capacity. From the figure it has shown that the plant efficiency is highest for the plant size of 8 MW.

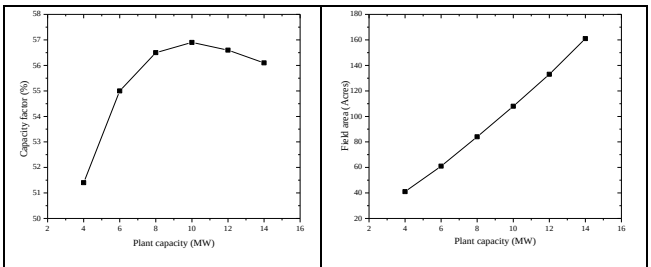


(a) Capacity factor with

(b) The floor spaces of the

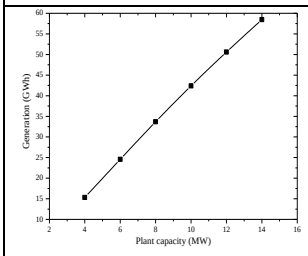


(c) Variation of electricity generation with plant capacity

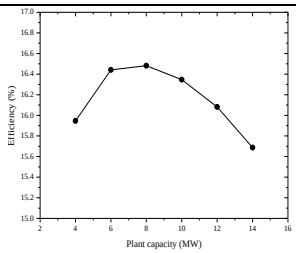


(d) Plant efficiencies at different plant capacities

**Fig. 8.** Plant capacity assessment

### 4.6 Plant performance analysis with respect to DNI

The scatter graph in Figure.9(a) displays the connotation between the DNI and the thermal power incident at the receiver surface. Thermal energy fall on the receiver surface likewise rises with increasing beam normal irradiance. DNI is being used as fuel in the CSP plant, which means that it is helping to produce energy. As can be seen in Figure.9 (b), the daily average maximum net power output grows as DNI rises. Monthly mean DNI vs net electricity production from the CSP plant is depicted in Figure.9(c). Every month of the year has satisfactory DNI levels for the research location, but September through December stand out as particularly high. Because of this, the plant's net electricity output goes way up during these months.

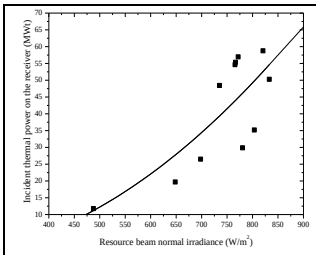


(a) Incident thermal power on the receiver vs resource beam normal irradiance.

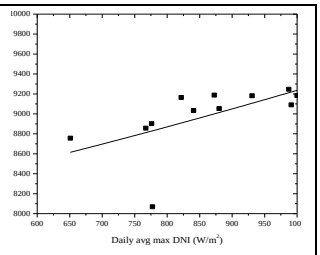


(b) Daily average max DNI versus daily average maximum net electricity output

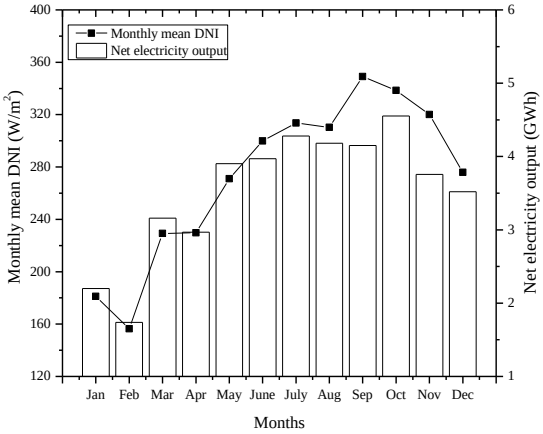


(c) Monthly net electricity output and direct normal irradiation

**Fig. 9.** DNI on plant performance

### 4.7 Power cycle performance

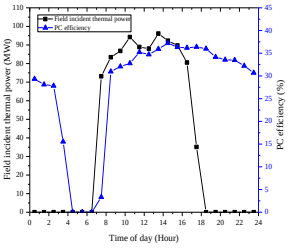


(a) Variation of the thermal power incident on the field and efficiency of the plant through out the year.

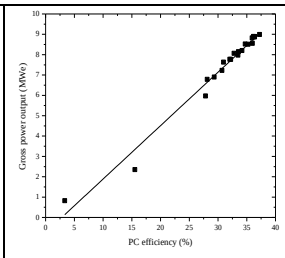


(b) Impact of PC efficiency on PC gross power output

**Fig. 10.** PC performance of the CSP plant

Figure.10 (a) displays the thermal power incident on the solar field and the power cycle efficiency of the studied STP through out the year. The power cycle performance efficiency rises with the growing thermal energy incident on the heliostat field. Figure.10 (b) illustrates the posistive relation between the power cycle efficiency and gross power output. Gross power output increases with the growth of the power cycle effic ciency.

### 4.8 Energy flow pattern

Solar power plant energy loss may be broken down by individual components with the use of an energy flow diagram. Figure.11 is an energy flow schematic for the 10 MW solar tower power station. It has been determined that each part contributes to the overall energy waste. The energy loss is highest for the power plant occur in the solar field (46.29%). The second highest losses happen in the power block which is 31.57%. The losses percentage in receiver is 5.33% of the entire power plant losses and other losses adds 0.46% of the entire losses which happen in pump, losses in pipe etc.

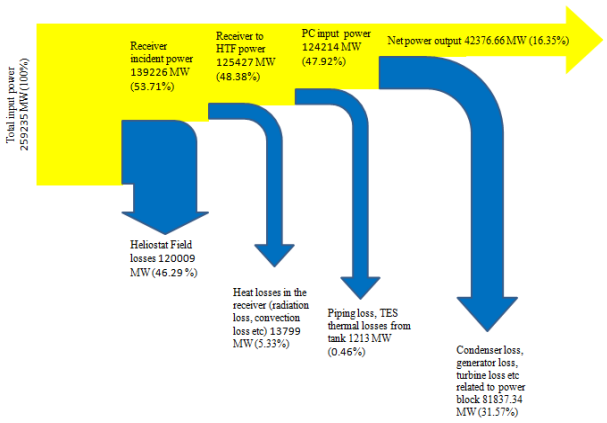


**Fig. 11** Flow chart of energy flow for 10 MW STP plant

### 4.9 Plant economics

The primary goal of a power plant economic assessment is, irrespective of funding options, to establish the project's intrinsic profitability. Project planners benefit from having a more full understanding of the project's potential constraints. The LCOE is the most useful parameters for evaluating economic analysis [44-50]. The whole lifetime power cost is determined by the LCOE method.

Figure.12 (a) shows that for a TES value of 10 hr and for a SM value of 2.4, the LCOE is observed the lowest (12.02 cent/kWh). Figure.12 (b) shows that the CSP size has a crucial influence on CSP LCOE. With the upper CSP capacity, the LCOE is observed to be lower. At lesser CSP size, the LCOE is found higher due to the lower annual electricity production.

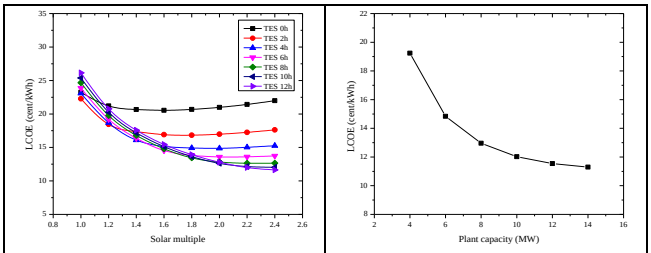


(a) Effect of SM on the LCOE for different value of TES.

(b) Effect of Plant capacity on the LCOE

**Fig. 12.** Economic evolution

## 5. Performative Comparison

**TABLE 2** Comparision of the plant performance

| Sl. No. | Normalized parameter | System performance | System performance with existing study | | |
|---|---|---|---|---|---|
| | | Obtained value | CSP technology | Value | Ref. |
| 1 | Plant capacity factor (%) | 56.90 | Solar tower power (STP) | 24 | [18] |
| | | | Parabolic trough (PT) | 21 | [18] |
| 2 | Plant efficiency (%) | 16.35 | STP | 13.5 | [22] |
| | | | PT | 21.3 | [4] |
| 3 | Land demand ($MW/km^2$) | 22.90 | STP | 20 | [18] |
| | | | PT | 47.3 | [18] |
| 4 | Water usage (litter/$MWh_e$/y) | 199.83 | PT | 2678.77 | [4] |
| 5 | Gross energy-to-net energy conversion | 88.66 | PT | 94.2 | [4] |
| 6 | Plant solar energy-to-electrical energy conversion (gross) | 18.44 | STP | 28.72 | [45] |
| | | | PT | 16 | [46] |
| 7 | LCOE ($/kWh) | 0.1202 | STP | 0.14 | [1] |
| | | | PT | 0.15 | [1] |

In this study, researchers analyse the effectiveness of a CSP plant with STP plant in a cold arid region with high intensities of DNI. Therefore, in order to evaluate the efficacy of the planned scheme, the study's findings are compared with those of the already-existing concentrated solar thermal system. Table 2 compares the existing studied solar thermal technologies with this study obtained results in terms of different comaparative normalized parameters, like power plant capacity factor, land requirement, plant solar to electric efficiency, power plant gross to net eelectrcity conversion efficiency,annual usage of water, LCOE etc..

## 6. Conclusion

When it comes to harnessing solar energy to produce electricity, cental tower technology of the CSP plant represent one of the most capable options of power production. This research aims to analyze the characterize of a solar thermal plant for a cold arid high DNI environment using a variety of analytical factors. Several important studies, such the impact of SM for soalr power production, impact of TES on power plant performance , central receiver performance analysis, effect of DNI over CSP plant energy production performance, and CSP economical analysis, have been conducted. According to the results, the LCOE is decreased and the power plant

capacity factor is increased when thermal energy storage is incorporated. Results show that the LCOE, plant efficiency, and capacity factor all come in at 0.1202 $/kWh, 16.35%, and 56.90%, respectively. A greater DNI correlates with increased plant efficiency, as shown in the study. It is also discovered that there is a close connection between SM, the TES and capacity factor. The LCOE is seen to decrease with increasing SM and TES. The heliostat solar field has the highest loss rate (46.29%), followed by the power block (31.57%). In this study it has been observed that the plant efficiency is the section where the researchers can work in the future because the field optical losses are huge for the particular study. Field optical efficiency has a big impact on the plant overall efficiency. By optimizing the solar field optical efficiency it can be possible to increase the plant performance. So from the study it has been observed that Leh Ladakh region is highly solar potential region in the India with huge amount of DNI which is ideal for solar tower type CSP plant. From the study analysis it has been observed that the CSP CF, and CSP generation is high and the LCOE is also very low for this region. With proper design and optimization of the design parameter the Leh Ladakh region will become the solar energy power hub for India.

## Reference


[1] Purohit I, Purohit P. Techno-economic evaluation of concentrating solar power generation in India. Energy Policy; 38: 3015-3029, 2010.

[2] Sharma C, Sharma AK, Mullic SC, Kandpal TC. Assessment of solar thermal power generation potential in India. Renewable and Sustainable Energy Reviews,; 42: 902-912, 2015.

[3] Renewable capacity statistics 2017 <http://www.irena.org/DocumentDownloads/Publications/IRENA_RE_Capacity_Statistics_2017>. [Accessed on 15th November 2017].

[4] Bishoyi D, Sudhakar K. Modeling and performance simulation of 100 MW PTC based solar thermal power plant in Udaipur India. Case Studies in Thermal Engineering,; 10: 216-226, 2017.

[5] Kaygusuz K. Prospect of concentrating solar power in Turkey: The sustainable future. Renewable and Sustainable Energy Reviews,; 15(1): 808-814, 2011 .

[6] Sharma NK, Tiwari PK, Sood YR. Solar energy in India: strategies, policies, perspectives and future potential. Renewable and Sustainable Energy Reviews,; 16: 933-941, 2012.

[7] Breyer C, Knies G. Global energy supply potential of concentrating solar power, In: Proceedings of the solar power and chemical energy systems. Berlin, September 2009.

[8] Ummadisingu A, Soni MS. Concentrating solar power – technology, potential and policy in India. Renewable and Sustainable Energy Reviews,; 15: 5169-5175, 2011.

[9] Peterseim JH, White S, Tadros A, Hellwig U. Concentrated solar power hybrid plants, which technologies are best suited for hybridisation? Renewable Energy,; 57: 520-532, 2013.

[10] Faraz T. Benefits of concentrating solar power over solar photovoltaic for power generation in Bangladesh. 2nd Int. Conf. on Developments in Renewable Energy Technology (ICDRET) 5-7 January 2012, Dhaka, Bangladesh.

[11] Arora PR. A Vital Role of Concentrating Solar Power Plants of Rajasthan in Future Electricity Demand of India. International Journal of Scientific and Research Publications,; 3(6): 1-7, 2013.

[12] Santra P, Scope of Solar Energy in Cold Arid Region of India at Leh Ladakh, Annals of Arid Zone 54(3&4): 109-117, 2015.

[13] Sahoo U, Kumar R, Pant PC, Chaudhary R. Resource assessment for hybrid solar-biomass power plant and its thermodynamic evaluation in India. Solar Energy,; 139: 47-57, 2016.

[14] Leh, https://en.wikipedia.org/wiki/Leh, accessed on 15th August 2022

[15] Hang Q, Juna Z, Xiao Y, Junkui C. Prospect of concentrating solar power in China—the sustainable future. Renewable and Sustainable Energy Reviews,; 12: 2505-2514, 2008.

[16] Charabi Y, Gastli A. GIS assessment of large CSP plant in Duqum, Oman. Renewable and Sustainable Energy Reviews,; 14: 835-841, 2010.

[17] Kuravi S, Trahan J, Goswami DY, Rahman MM, Stefanakos EK. Thermal energy storage technologies and systems for concentrating solar power plants. Progress in Energy and Combustion Science,; 39: 285-319, 2013.

[18] Ramdé EW, Azoumah Y, Hammond AB, Rungundu A, Tapsoba G. Site Ranking and Potential Assessment for Concentrating Solar Power in West Africa. Natural Resources,; 4: 146-153, 2013.

[19] Benammar S, Khellaf A, Mohammedi K. Contribution to the modeling and simulation of solar power tower plants using energy analysis. Energy Conversion and Management,; 78: 923-930, 2014 .

[20] Turchi CS, Ma Z. Co-located gas turbine/solar thermal hybrid designs for power production. Renewable Energy,; 64: 172-179, 2014.

[21] Yu Q, Wang Z, Xu E. Analysis and improvement of solar flux distribution inside a cavity receiver based on multi-focal points of heliostat field. Applied Energy,; 136: 417-430, 2014.

[22] Boudaoud B, Khellaf A, Mohammedi K, Behar O. Thermal performance prediction and sensitivity

analysis for future deployment of molten salt cavity receiver solar power plants in Algeria. Energy Conversion and Management,; 89: 655-664, 2015.

[23] Liu SJ, Faille D, Fouquet M, Hefni BE, Wang Y, Zhang JB, Wang ZF, Chen GF, Soler R. Dynamic simulation of a 1MWe CSP tower plant with two-level thermal storage implemented with control system. Energy Procedia,; 69: 1335-1343, 2015.

[24] Mutuberria A, Pascual J, Guisado MV, Mallor F. Comparison of heliostat field layout design methodologies and impact on power plant efficiency. Energy Procedia,; 69: 1360-1370, 2015.

[25] Santos MJ, Merchán RP, Medina A, Hernández AC. Seasonal thermodynamic prediction of the performance of a hybrid solar gas-turbine power plant. Energy Conversion and Management,; 115: 89-102, 2016.

[26] Trabelsi SE, Chargui R, Qoaider L, Liqreina A, Guizani AA. Techno-economic performance of concentrating solar power plants under the climatic conditions of the southern region of Tunisia. Energy Conversion and Management,; 119: 203-214, 2016.

[27] Astolfi M, Binotti M, Mazzola S, Zanellato L, Manzolini G. Heliostat aiming point optimization for external tower receiver. Solar Energy,; 157: 1114-1129, 2017.

[28] Bhattacharjee R, Bhattacharjee S. Viability of a concentrated solar power system in a low sun belt prefecture. Front. Energy (Springer), Vol. 14, pp-850–866, 2020.

[29] Bhattacharjee R, Bhattacharjee S, Performance of inclined heliostat solar field with solar geometrical factors, Energy Sources, Part A: Recovery, Utilization, and Environmental Effects (Taylor and Francis), (2020) DOI:10.1080/15567036.2020.1784318.

[30] Lisbona P, Bailera M, Hills T, Sceats M, Díez L.I, Romeo L.M, Energy consumption minimization for a solar lime calciner operating in a concentrated solar power plant for thermal energy storage. Renewable Energy 156 (2020) 1019e1027.

[31] Ma Z, Li M.J, Zhang K.M, Yuan F, Novel designs of hybrid thermal energy storage system and operation strategies for concentrated solar power plant, Energy (2020), doi.org/10.1016/j.energy.2020. 119281.

[32] Middelhoff E, Furtado L.A., Peterseim J.H, Madden B, Ximenes F, Florin N, Hybrid concentrated solar biomass (HCSB) plant for electricity generation in Australia: Design and evaluation of techno-economic and environmental performance, Energy Conversion and Management 240 (2021) 114244.

[33] Coutinho D.P.A, Rodrigues J.A.M.M, Santos A.J.P, Semiao V.S.A, Thermoeconomic analysis and optimization of a hybrid solar-thermal power plant using a genetic algorithm, Energy Conversion and Management 247 (2021) 114669.

[34] Tiwari V, Rai A.C, Srinivasan P, Parametric analysis and optimization of a latent heat thermal energy storage system for concentrated solar power plants under realistic operating conditions, Renewable Energy 174 (2021) 305-319.

[35] Boukelia T.E, Arslan O, Bouraoui A, Thermodynamic performance assessment of a new solar tower-geothermal combined power plant compared to the conventional solar tower power plant, Energy 232 (2021) 121109.

[36] Liu M, Riahi S, Jacob R, Belusko M, Bruno F, Design of sensible and latent heat thermal energy storage systems for concentrated solar power plants: thermal performance analysis, Renewable Energy (2020), DOI: https://doi.org/10.1016/j.renene.2019.11.115.

[37] García-Ferrero J, Merchán R.P, Santos M.J, Medina A, Hernández A.C, Brayton technology for Concentrated Solar Power plants: Comparative analysis of central tower plants and parabolic dish farms, Energy Conversion and Management 271 (2022) 116312.

[38] Collado FJ, Guallar J. Two-stages optimised design of the collector field of solar power tower plants. Solar Energy,; 135: 884-896, 2016.

[39] Habte A, Sengupta M, Lopez A. Evaluation of the National Solar Radiation Database (NSRDB): 1998-2015. < https://www.nrel.gov/ docs/ zfy17osti/67722.pdf>. [Accessed on 26th September 2018]

[40] Pozivil P, Ackermann S, Steinfeld A. Numerical Heat Transfer Analysis of a 50 kWth Pressurized-Air Solar Receiver. Journal of Solar Energy Engineering,; 137: 1-4, 2015.

[41] Wagner MJ. Simulation and Predictive Performance Modeling of Utility-Scale Central Receiver System Power Plants. University of Wisconsin – Madison 2008; 1-259.

[42] Guédez R, Ferruzza D. Thermocline Storage for Concentrated Solar Power Techno-economic performance evaluation of a multi-layered single tank storage for Solar Tower Power Plant, KTH School of Industrial Engineering and Management 2015.

[43] Walter S, Daniel J. Packey, Thomas H. A Manual for the Economic Evaluation of Energy Efficiency and Renewable Energy Technologies. National Renewable Energy Laboratory 1995.

[44] Branker K, Pathak MJM, Pearce JM. A review of solar photovoltaic levelized cost of electricity. Renewable and Sustainable Energy Reviews,; 15(9): 4470-4482, 2011.

[45] Concentrating Solar Power Projects - Ivanpah Solar Electric Generating System, Concentrating Solar Power, NREL.

<https://www.nrel.gov/csp/solarpaces/project_detail.cfm/projectID=62>. [Accessed on 19th June 2017].

[46] Concentrating Solar Power Projects - Andasol-1, Concentrating Solar Power, NREL. <https://www.nrel.gov/csp/solarpaces/project_detail.cfm/projectID=3>. [Accessed on 19th June 2017].

[47] Yaseen, M., Hayder Sabah Salih, Mohammad Aljanabi, Ahmed Hussein Ali, & Saad Abas Abed. (2023). Improving Process Efficiency in Iraqi universities: a proposed management information system. Iraqi Journal For Computer Science and Mathematics, 4(1), 211–219. https://doi.org/10.52866/ijcsm.2023.01.01.0020

[48] Aljanabi, M. ., & Sahar Yousif Mohammed. (2023). Metaverse: open possibilities. Iraqi Journal For Computer Science and Mathematics, 4(3), 79–86. https://doi.org/10.52866/ijcsm.2023.02.03.007

[49] Atheel Sabih Shaker, Omar F. Youssif, Mohammad Aljanabi, ABBOOD, Z., & Mahdi S. Mahdi. (2023). SEEK Mobility Adaptive Protocol Destination Seeker Media Access Control Protocol for Mobile WSNs. Iraqi Journal For Computer Science and Mathematics, 4(1), 130–145. https://doi.org/10.52866/ijcsm.2023.01.01.0011

[50] Hayder Sabah Salih, Mohanad Ghazi, & Aljanabi, M. . (2023). Implementing an Automated Inventory Management System for Small and Medium-sized Enterprises. Iraqi Journal For Computer Science and Mathematics, 4(2), 238–244. https://doi.org/10.52866/ijcsm.2023.02.02.021

[51] Ashok Kumar, L. ., Jebarani, M. R. E. ., & Gokula Krishnan, V. . (2023). Optimized Deep Belief Neural Network for Semantic Change Detection in Multi-Temporal Image. International Journal on Recent and Innovation Trends in Computing and Communication, 11(2), 86–93. https://doi.org/10.17762/ijritcc.v11i2.6132

[52] Wang Wei, Natural Language Processing Techniques for Sentiment Analysis in Social Media , Machine Learning Applications Conference Proceedings, Vol 1 2021.

[53] Pandey, J.K., Ahamad, S., Veeraiah, V., Adil, N., Dhabliya, D., Koujalagi, A., Gupta, A. Impact of call drop ratio over 5G network (2023) Innovative Smart Materials Used in Wireless Communication Technology, pp. 201-224.